

Supplementary Information

A deep conical agarose microwell array for adhesion independent three-dimensional cell culture and dynamic volume measurement

Andreas R. Thomsen^{*a,b,c}, Christine Aldrian^{a,b,c}, Peter Bronsert^{b,c,d,e}, Yi Thomann^f, Norbert Nanko^{a,c}, Nicolas Melin^g, Gerta Rücker^{c,h}, Marie Follo^{c,i}, Anca L. Grosu^{a,b,c}, Gabriele Niedermann^{a,b,c}, Paul G. Layer^j, Anja Heselich^k and Per G. Lund^{*a,c}

^aDepartment of Radiation Oncology, Medical Center – University of Freiburg, Germany.

^bGerman Cancer Consortium (DKTK), Partner Site Freiburg and German Cancer Research Center (DKFZ), Heidelberg, Germany.

^cFaculty of Medicine, University of Freiburg, Germany

^dInstitute for Surgical Pathology, Medical Center – University of Freiburg, Germany

^eComprehensive Cancer Center Freiburg, Medical Center – University of Freiburg, Germany

^fFreiburg Material Research Center and Institute for Macromolecular Chemistry, Department of Chemistry, University of Freiburg, Germany

^gVisceral and Transplantation Surgery, Department of Clinical Research, University of Bern, Switzerland

^hInstitute for Medical Biometry and Statistics, Medical Center – University of Freiburg, Germany.

ⁱDepartment of Hematology/Oncology, Medical Center – University of Freiburg, Germany.

^jDevelopmental Biology & Neurogenetics, Faculty of Biology, Technical University of Darmstadt, Germany.

^kDepartment for Biophysics, GSI Helmholtz Center for Heavy Ion Research, Darmstadt, Germany.

*E-mail: andreas.thomsen@uniklinik-freiburg.de and/or per.lund@uniklinik-freiburg.de

		CAMA 1x1		CAMA 2x2	
distances		mean [μm]	SD	mean [μm]	SD
	peak to peak	999.87	± 5.15	2005.11	± 5.27
	center to center	1000.97	± 5.7	1991.62	± 9.69
	highest diameter (2R)	830.25	± 7.22	852.35	± 7.69
	lowest diameter (2r)	237.48	± 4.76	254.8	± 4.09
	microwell depth (H+h)	1772.41	± 10.1	1776.16	± 10.2
	microwell bottom thickness	408.95	± 37.6	289.8	± 28.2
angles		mean [$^\circ$]	SD	mean [$^\circ$]	SD
	upper opening angle (2ω)	115.96	± 1.97	112.12	± 0.47
	lower opening angle (2φ)	19.95	± 0.29	19.95	± 0.35

Table S1

Dimensions of the CAMA (conical agarose microwell array, as indicated in Figure 1 were measured repeatedly ($n \geq 20$ separate measurements) and are indicated as mean with Standard Deviation (SD). "Peak to peak" is the distance measured between the highest points between two microwells, while "center to center" refers to the distance measured between the two lowest points at the bottom of two microwells.

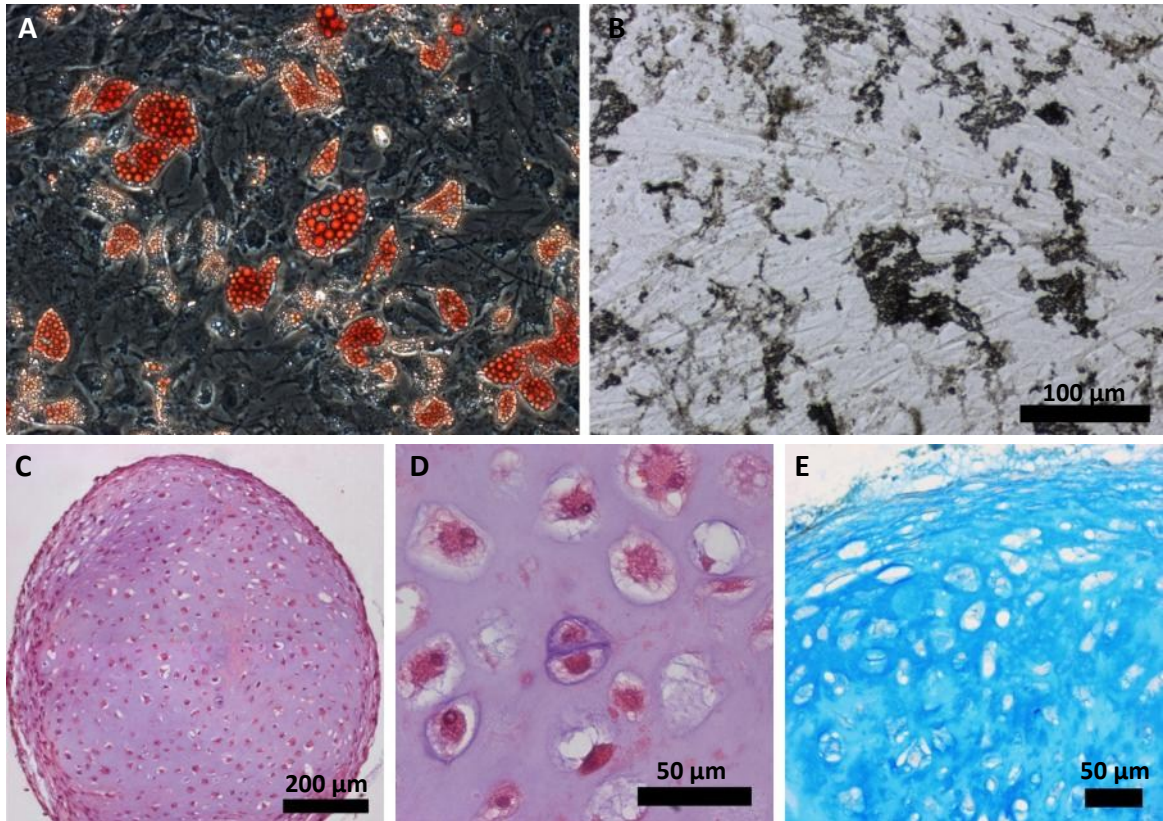


Figure S1 Functional validation of human bone marrow-derived MSC

(A) For adipogenic differentiation, subconfluent monolayers were incubated in AdipoDiff medium (Miltenyi) and stained for lipid droplets using Oil Red O (Chroma) after two weeks.

(B) For osteogenic differentiation, subconfluent monolayers were kept in osteogenic medium (DMEM/F12 with 5% human serum, 52 mg/L ascorbic acid 2-phosphate, 10 mM β -glycero phosphate, 10^{-7} M dexamethasone, and 230 mg/L CaCl_2) for two weeks and then stained for extracellular mineral using the von Kossa method.

(C-E) For chondrogenic differentiation, MSCs were suspended in ChondroDiff medium (Miltenyi) and seeded into large conical agarose microwells at a density of 180000 cells per microwell. After 22 days in ChondroDiff medium, spheroids were fixated and embedded for paraffin histology. Sections from the same spheroid demonstrate formation of hyaline-like cartilage. (C)+(D) H&E staining, (E) alcian blue staining.

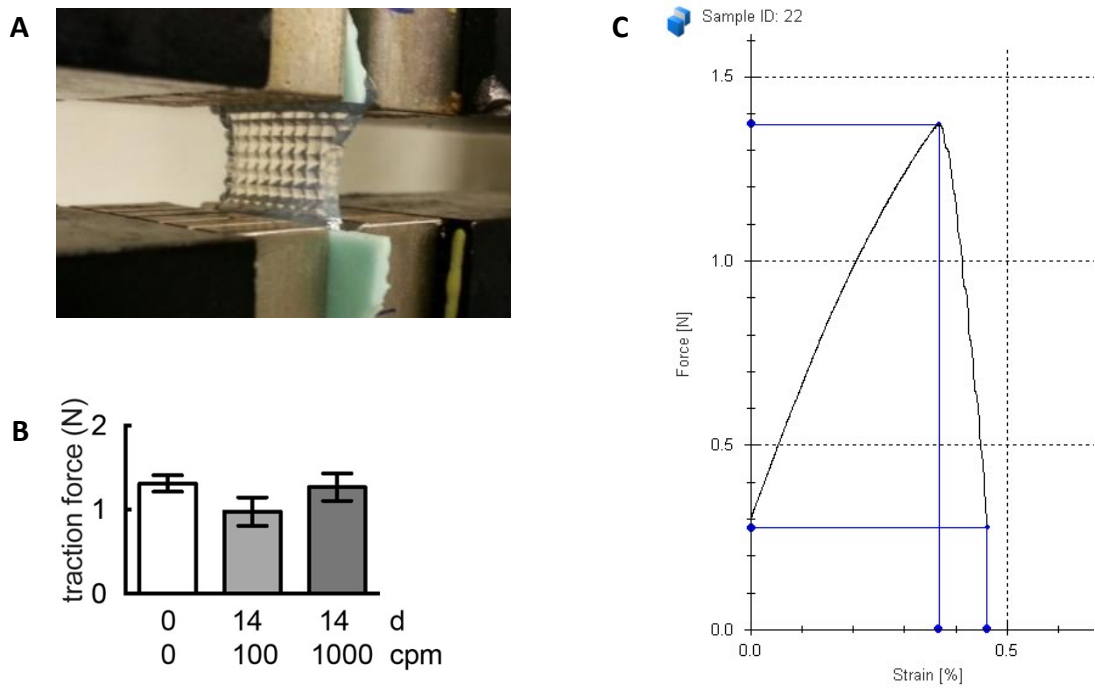


Figure S2 Mechanical stability of the CAMA

(A) Setup of strain test with CAMA clamped into the material testing machine. (B) The traction force [N] needed to tear apart the 2 mm CAMA is compared under cell culture conditions (grey bars) and non-cell culture conditions (white bar). The number of cells seeded per microwell (cpm) and the days (d) in culture are indicated. (C) Typical traction curve obtained by material testing of the CAMA.

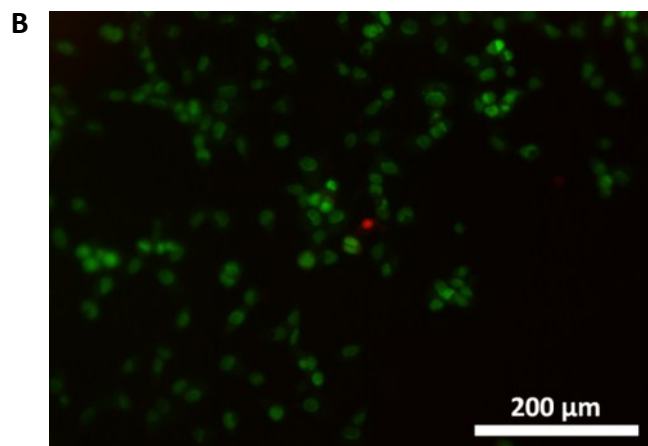
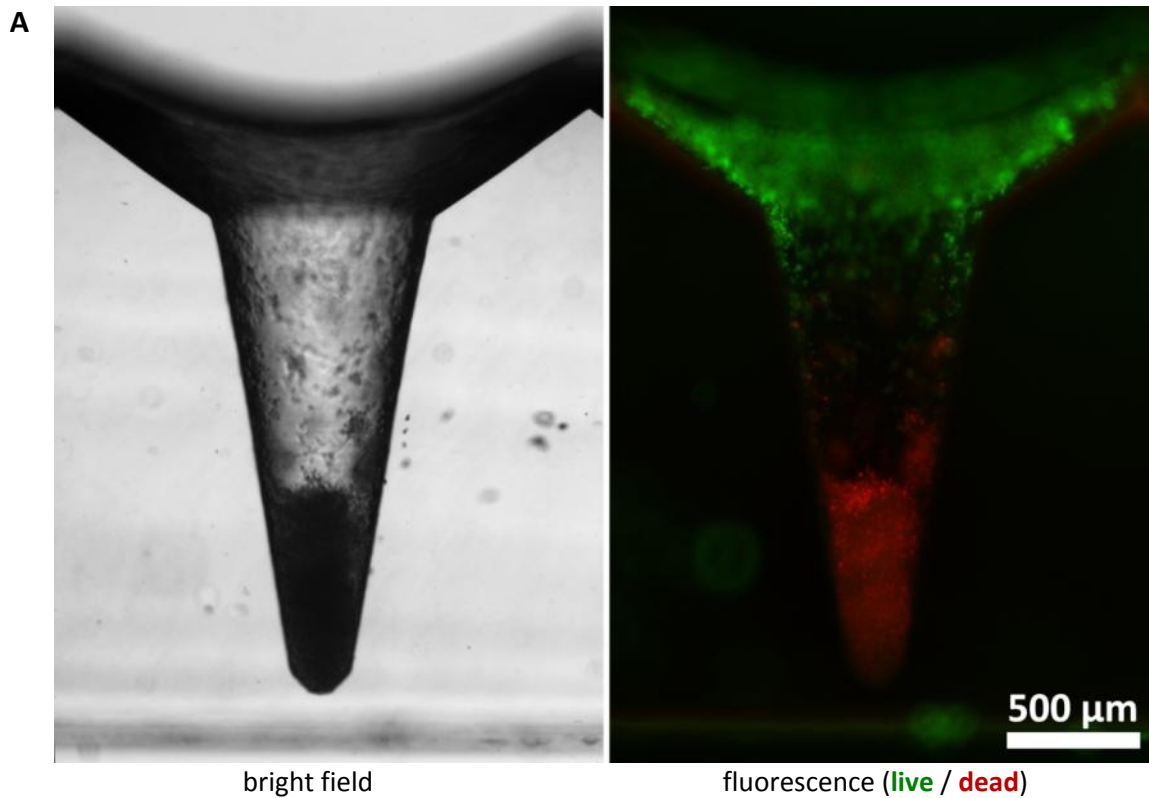


Figure S3 Deep conical microwells from non-permeable material show limited supply of cells

(A) Using the replica moulding technique shown in Fig. 1, deep conical microwells may also be made from transparent polydimethylsiloxane (PDMS, Wacker Chemie, Germany). However, cells located at the bottom of such non-permeable microwells are likely to die from shortage of nutrients, while cell viability increases towards the opening of the microwell. (B) The PDMS material itself does not impair cell viability, as seen with cells seeded on a planar PDMS surface. Both show live/dead staining with Syto 16 (viable cells, green) and propidium iodide (dead cells, red). Panc-1 cells, day 7.

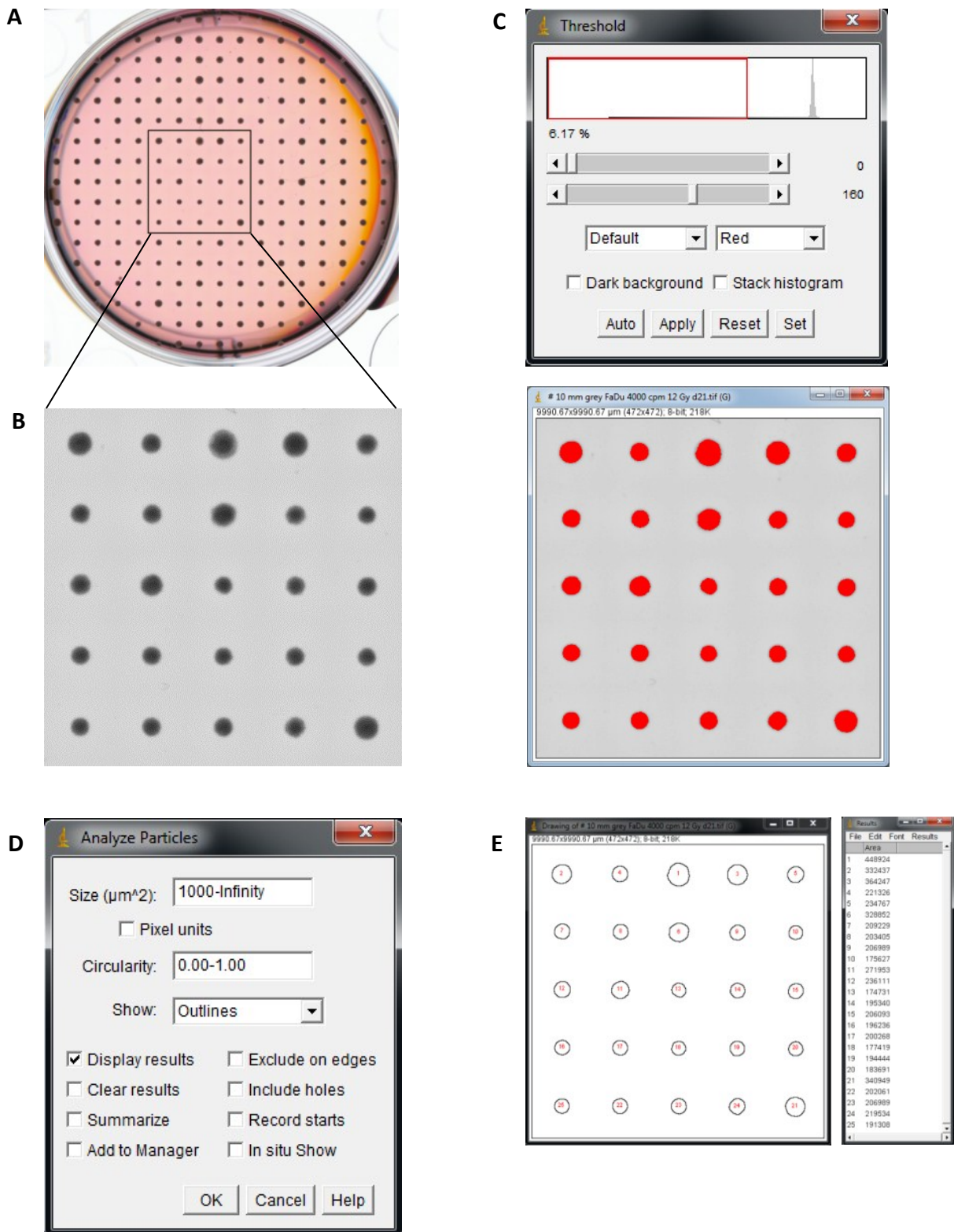


Figure S4 Cell aggregate volume measurement using Image J

FaDu squamous cell carcinoma cells were seeded at 4000 cells per microwell (cpm) into the CAMA and irradiated with 12 Gy on day 6. (A) Transmitted light scan obtained on day 21. (B) Greyscale clipping of 10 x 10 mm. (C) Application of a threshold to display the cell aggregate margin. (D) Settings for image analysis. A minimal area of 1000 μm^2 is applied to exclude artefacts as dust particles etc. (E) Output of measurements. The raw values of the projected area [μm^2] are then converted into cell aggregate volumes [μm^3] as shown in Figure S5.

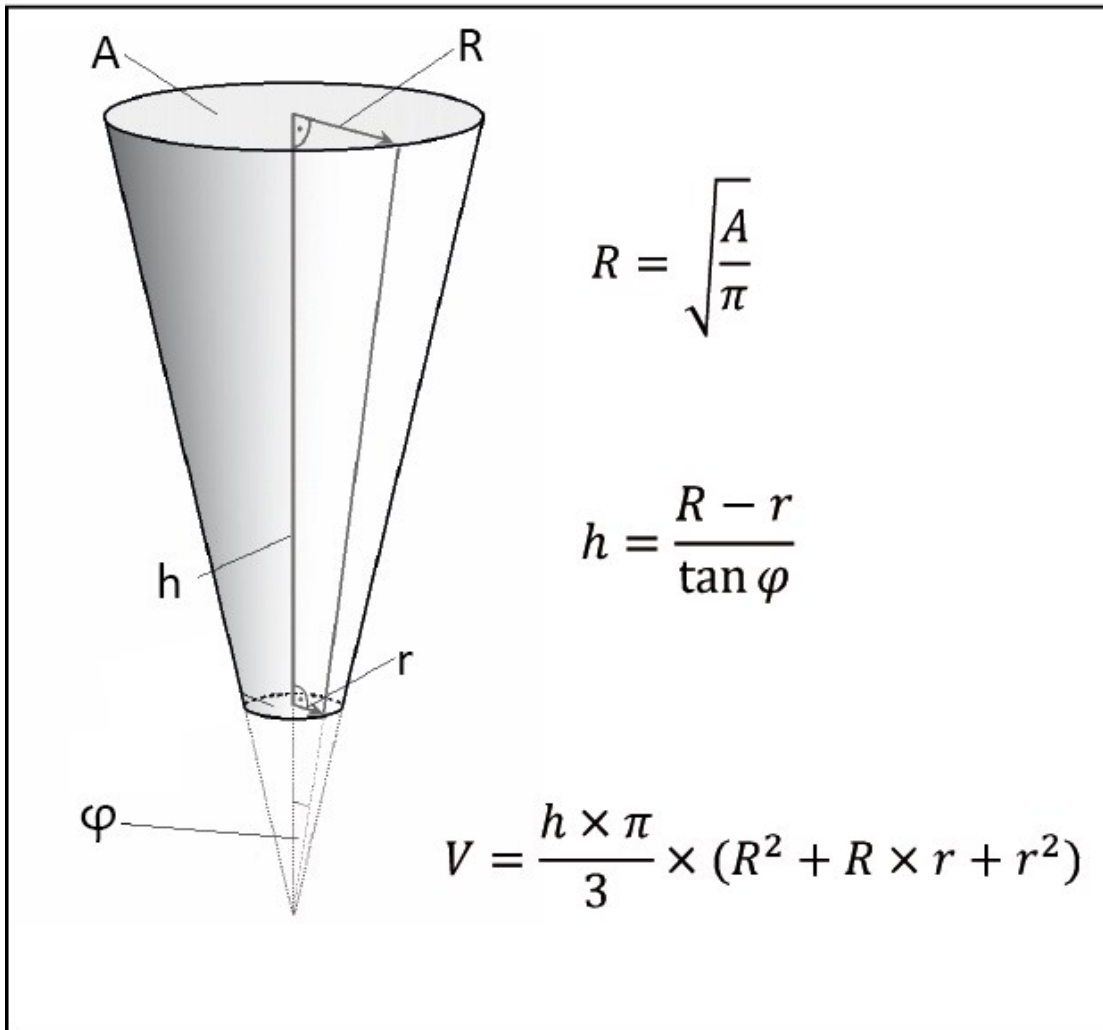
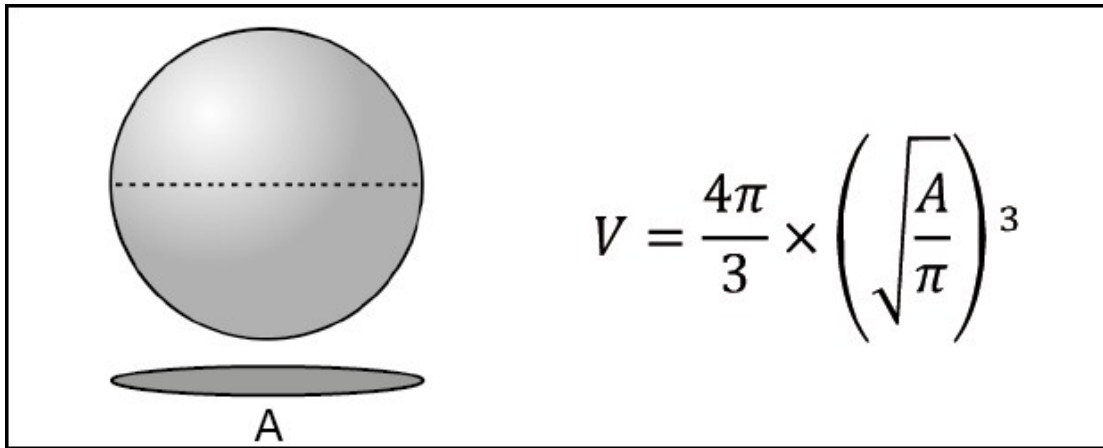
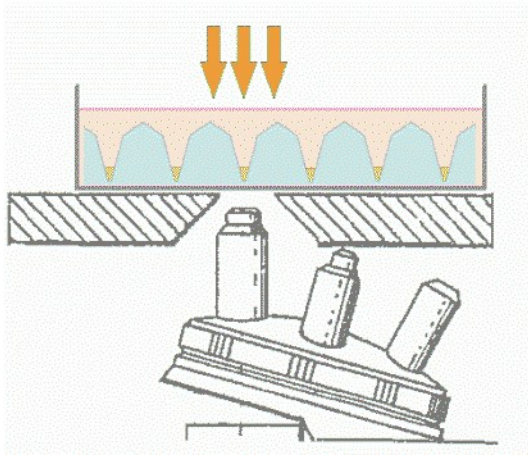
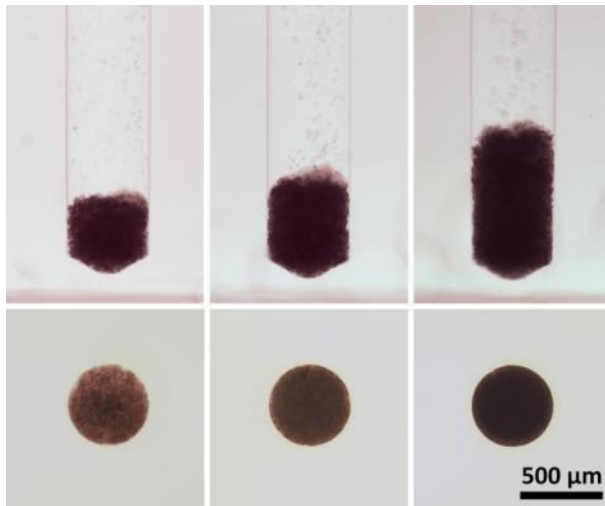


Figure S5 Formulas for calculation of the spheroid and conical cell aggregate volume

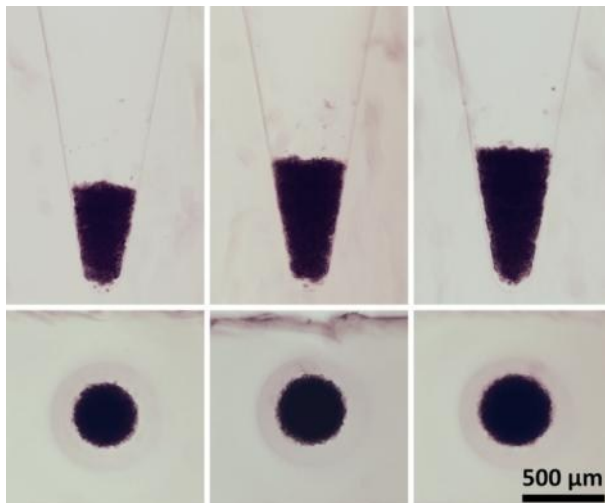
The volume of a sphere is easily calculated given the projected area A. A corresponds to the area with the largest diameter of the spheroid (upper box).

The volume of a cone is calculated in three steps given the projected area A (lower box). A corresponds to the largest diameter of the conical cell aggregate. Following calculation of R, the height h of the conical cell aggregate is calculated using the given numbers of the lower radius (r) and the opening angle of the cone (φ). The volume of the conical cell aggregate is then calculated with the constant r and the calculated values of R and h. The volume of the rounded bottom ($1.68 \times 10^6 \mu\text{m}^3$) (see Fig.1 D) is finally added to the calculated volume.

A**B**

Side view

Bottom view

C

Side view

Bottom view

Figure S6 Conical microwells enable measurement of cell aggregate volume

(A) Cell aggregates are usually seen from the bottom of a microwell using an inverted microscope or an optical scanner. (B) In cylindrical microwells seen from the bottom, the projected area of the cell aggregates remains constant, irrespective from the filling level. (C) In contrast, in conical microwells seen from the bottom, the projected area of the cell aggregates increases with the filling level.



Figure S7 Photograph of the CAMA embedded into paraffin and cast into a block

For better visualisation, cell aggregates were stained with haematoxylin after formalin fixation and before further processing as displayed in Fig. 3.

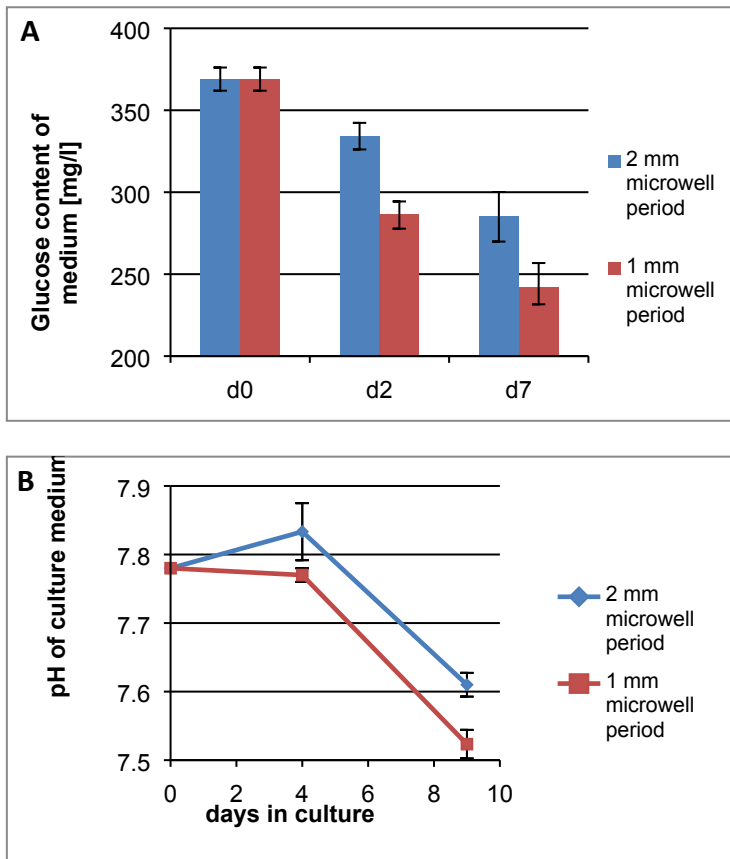


Figure S8 Metabolic assessment of MIA-PaCa 2 cell aggregates in different microwell spacing

(A) During cultivation, the glucose content of culture medium decreases more rapidly with the 1 mm microwell period, compared to the 2 mm microwell spacing. Data are means \pm SD, (n=5).

(B) Culture medium shows a trend towards lower pH values with the 1 mm microwell period. This suggests that both nutrient shortage and accumulation of waste products might play a role in reduced proliferation under a high density of microwells/cm². Data are means \pm SD, (n=3).

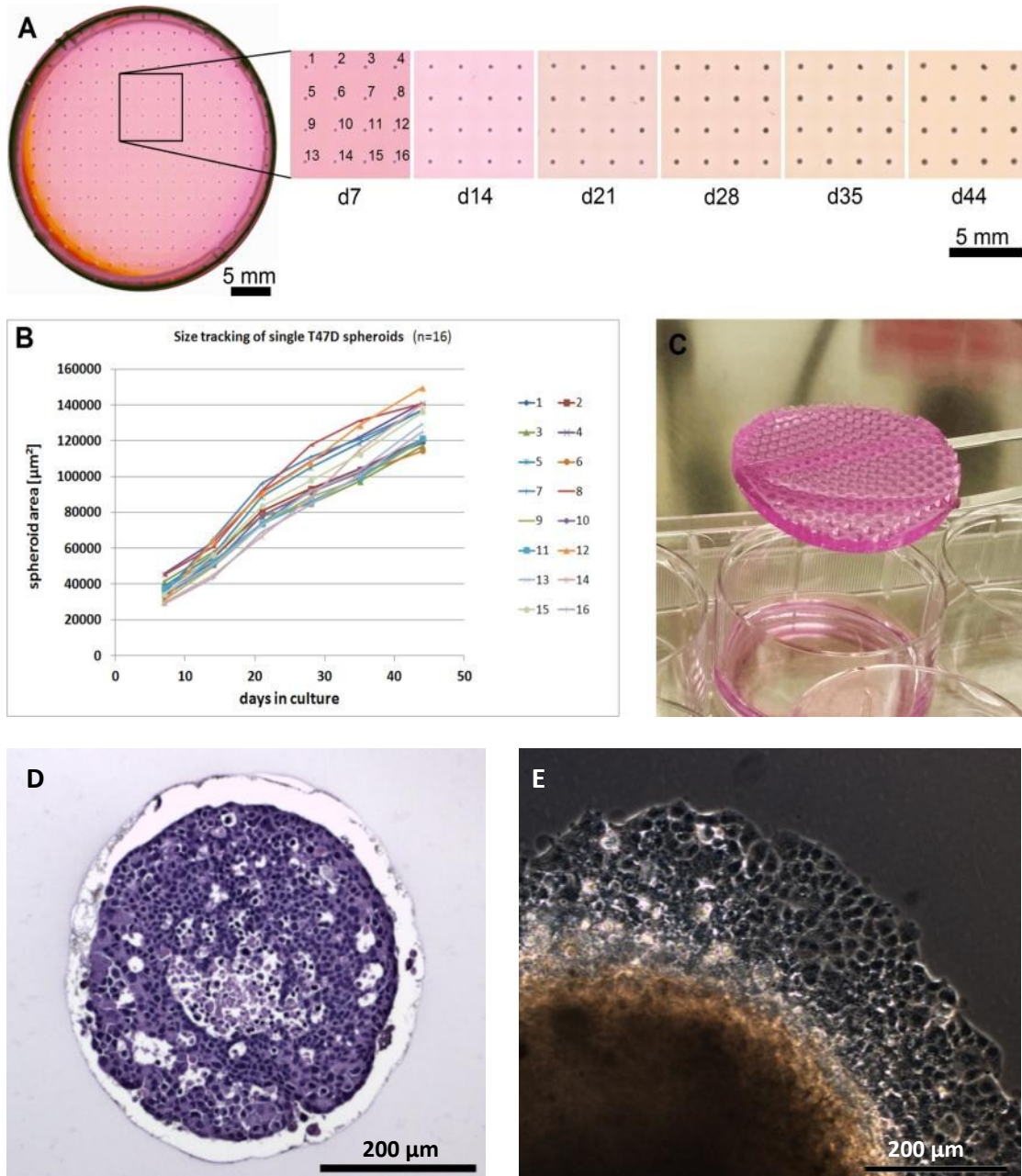


Figure S9 Long-term culture of multicellular tumour spheroids in CAMA

(A) Tracking growth of individual spheroids by repeated scanning. Square clippings show the same array region with 16 agarose microwells each initially seeded with approx. 1000 T47D human breast cancer cells. Spheroids were numbered consecutively as shown on d7. (B) Individual growth curves of all 16 spheroids obtained by image analysis within the square clippings. (C) After > 6 weeks of culture, the agarose microwell arrays retain stability and may be lifted out of 6-well-plate for further processing. (D) Paraffin section of a T47D spheroid after > 6 weeks of cultivation in CAMA. (E) Outgrowth of cells from T47D spheroid transferred into 2D culture after > 6 weeks of cultivation in CAMA.

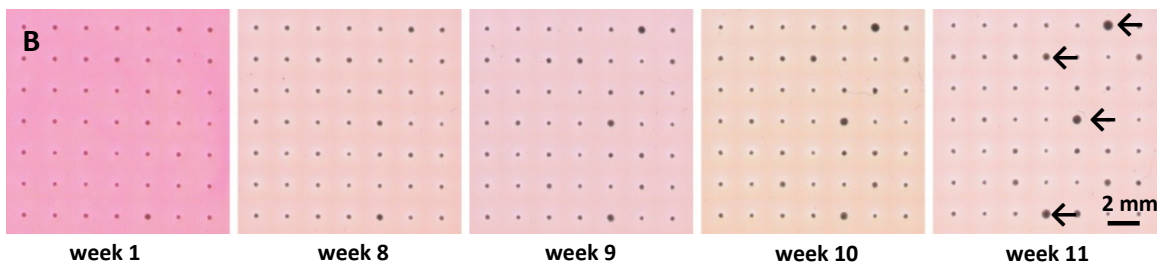
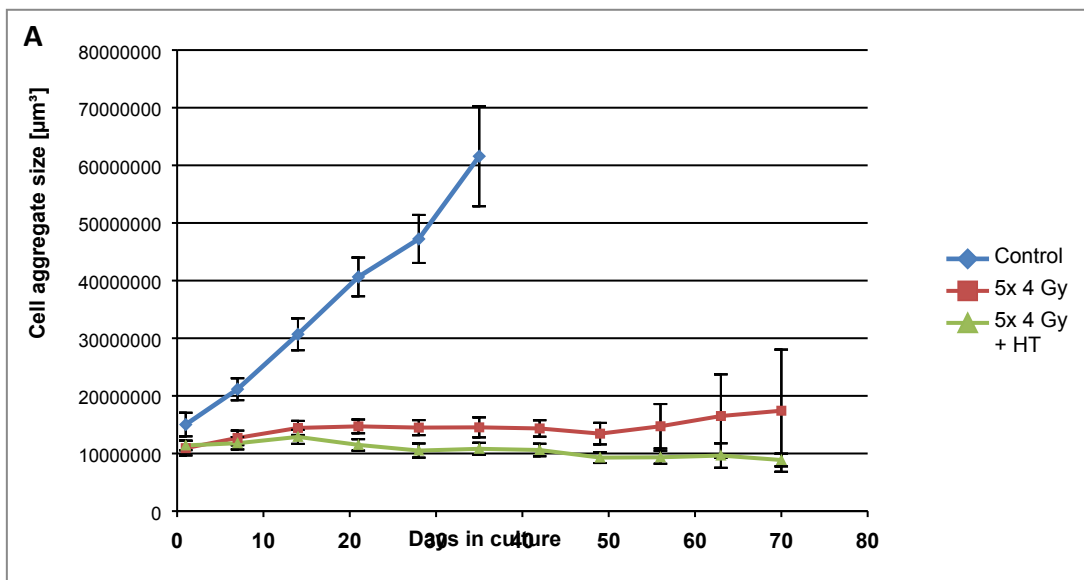


Figure S10 Size tracking of cell aggregates after hypofractionated irradiation +/- hyperthermia
 T47D human breast cancer cells were cultured as multicellular aggregates in CAMA and treated once weekly with hyperthermia at 42°C for 1 hour +/- irradiation of 4 Gy to a cumulative dose of 20 Gy. Response to treatment was monitored by repeated cell aggregate volume measurement for a total of 11 weeks. (A) Growth curves were plotted from data of 200 cancer cell aggregates for each treatment condition. Data are means \pm SD. (B) Clippings of scans with 49 cell aggregates in the "irradiation only" group show the recovery of single cell aggregates (\leftarrow), which re-grow several weeks after termination of treatment, resembling early tumour recurrences in the clinical setting. Such "rare events" may only be captured with large replicates in each treatment condition.

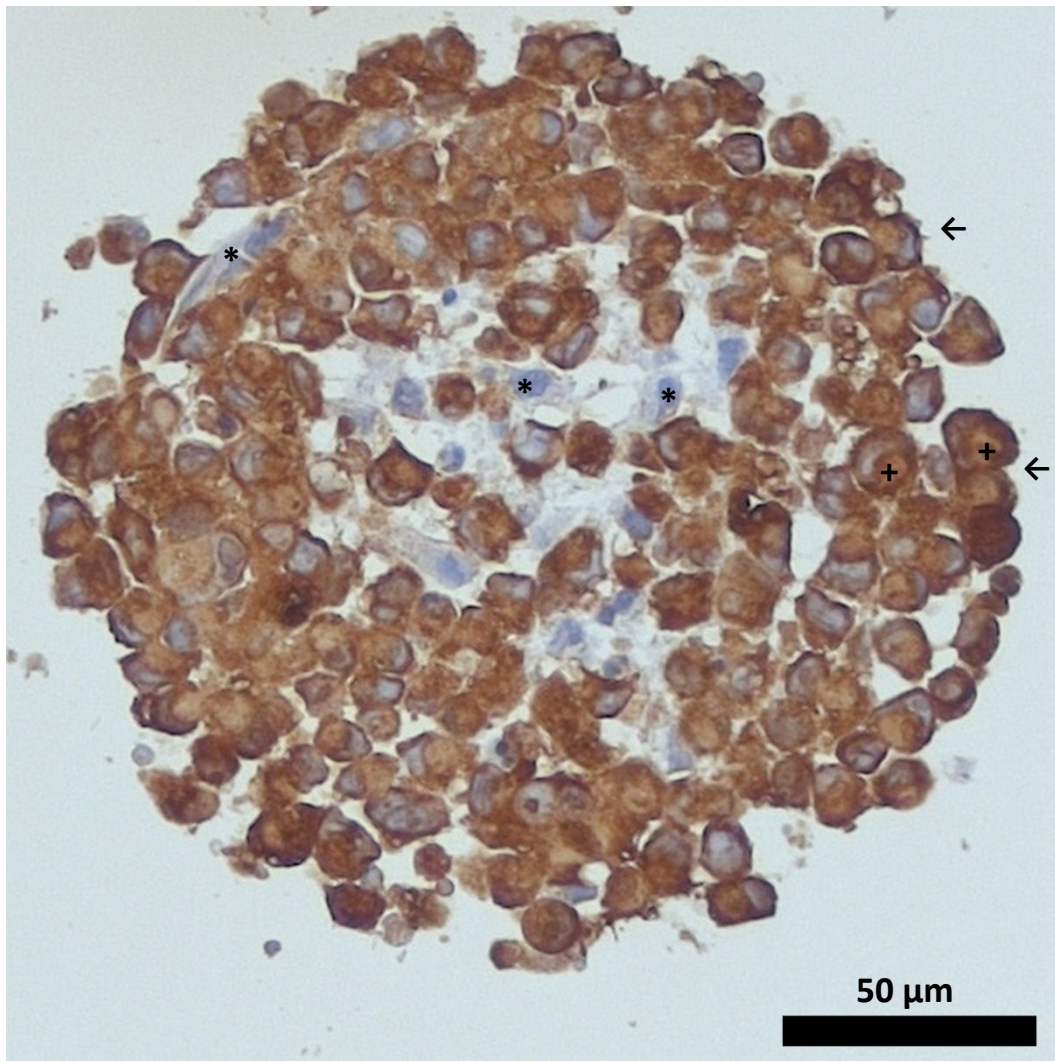


Figure S11 Cell arrangement and proliferation in contact co-culture of cancer and stromal cells

To create contact co-cultures of MIA PaCa-2 pancreatic adenocarcinoma cells with human bone marrow-derived MSCs in CAMA, a mixed cell suspension of cancer and stromal cells was adjusted to a seeding density of each 1000 cells per microwell. This paraffin section of d7 shows immunohistochemical staining of cytokeratin (clone AE1/AE3), which generates cytoplasmic staining in cells of epithelial origin, and of MIB-1 (Ki-67), which generates a nuclear signal in proliferating cells. Blue counterstaining with haematoxylin.

MIA PaCa-2 cells, being positive for cytokeratin (←), comprise the majority of cells and show a high fraction of proliferating cells with a nuclear signal for MIB-1 (+). The remaining cells, being cytokeratin-negative, represent the stromal cells, which are mainly positioned in the aggregate centre and stain negative for MIB-1 (*). This suggests that only the MIA PaCa-2 cancer cells cause cell aggregate growth, while the bone marrow-derived MSC do not contribute to an increase in volume.